Developmental Cell, Vol. 1, 435–440, September, 2001, Copyright ©2001 by Cell Press

The Arterial Pole of the Mouse Heart Forms from *Fgf10*-Expressing Cells in Pharyngeal Mesoderm

Robert G. Kelly,[1,3] Nigel A. Brown,[2] and Margaret E. Buckingham[1,3]
[1] CNRS URA 1947
Département de Biologie Moléculaire
Institut Pasteur
75724 Paris Cedex 15
France
[2] Department of Anatomy
and Developmental Biology
St. George's Hospital Medical School
London SW17 0RE
United Kingdom

Summary

Development of the arterial pole of the heart is a critical step in cardiogenesis, yet its embryological origin remains obscure. We have analyzed a transgenic mouse line in which β-galactosidase activity is observed in the embryonic right ventricle and outflow tract of the heart and in contiguous splanchnic and pharyngeal mesoderm. The *nlacZ* transgene has integrated upstream of the fibroblast growth factor 10 (*Fgf10*) gene and comparison with the expression pattern of *Fgf10* in pharyngeal mesoderm indicates transgene control by *Fgf10* regulatory sequences. DiI labeling shows a progressive movement of cells from the pharyngeal arch region into the growing heart tube between embryonic days 8.25 and 10.5. These data suggest that arterial pole myocardium originates outside the classical heart field.

Introduction

Vertebrate heart development initiates with the migration of cardiac precursors to the anterior lateral region of the embryo and the differentiation of cardiomyocytes within splanchnic mesoderm (see Fishman and Chien, 1997). Morphogenesis of the splanchnic epithelium at the time of foregut invagination generates a heart tube with a caudal venous pole and rostral arterial pole. As the heart tube closes dorsally, the ventricular region loops to the right and the venous pole is displaced rostrally behind the ventricles. During this process, the heart tube grows in length extremely rapidly (over 4-fold between embryonic days [E] 8 and 9 in the mouse) through the addition of extracardiac cells to the poles. At the arterial pole of the mouse heart, splanchnic epithelial cells continue to transform into cardiomyocytes during E9 to give rise to the distal outflow tract (OFT; Viragh and Challice, 1973). BMPs, which promote cardiomyogenesis (Schultheiss et al., 1997), are expressed in arterial pole myocardium at this stage (Jones et al., 1991). The distal OFT is also a late-added component of the chick heart, appearing substantially after looping (de la Cruz et al., 1977).

Despite the fact that OFT development and septation are critical steps in the establishment of the circulatory system, the origins of OFT myocardial precursor cells and the processes involved in extension of the arterial pole of the heart remain unknown. Here, we analyze a transgenic mouse line in which β-galactosidase activity, due to a position effect, is observed at E9.5 in the right ventricle, OFT, and splanchnic and pharyngeal mesoderm contiguous to OFT myocardium. This transgene has integrated upstream of the fibroblast growth factor 10 gene (*Fgf10*), and the expression pattern of *Fgf10* in pharyngeal mesoderm indicates that the *nlacZ* transgene is under transcriptional control of *Fgf10* regulatory sequences. Comparison of *Fgf10* and transgene expression patterns, together with DiI labeling of cultured mouse embryos, suggests that there is a continuous movement of myocardial precursor cells from the pharyngeal mesoderm into the arterial pole of the heart during OFT morphogenesis.

Results

The pattern of β-galactosidase activity in the *Mlc1v-nlacZ-24* transgenic mouse line is presented in Figure 1. At E9.5, β-galactosidase activity is observed in the myocardium of the OFT and embryonic right ventricle (Figures 1A, 1B, 1D, and 1E). Transgene expression is also observed in the pharyngeal region, including the mesodermal core of the branchial arches and the splanchnic epithelial dorsal wall of the pericardial cavity. This extracardiac expression domain is contiguous to OFT myocardial cells across the mesothelial wall of the aortic sac (Figures 1B and 1E). Genes encoding cardiac differentiation markers, including α-*cardiac actin*, are expressed in OFT myocardium but not in the dorsal pericardial wall or branchial arch mesoderm (Figure 1C). Other sites of transgene expression include endothelial cells in the distal OFT and arch arteries, the developing thyroid, limb bud mesenchyme, the posterior pituitary, and mesenchymal cells associated with endodermal derivatives including the lung, stomach, and pancreas (Figure 1).

The extracardiac domain of transgene expression contiguous to the distal end of the OFT is highly dynamic between E8.5 and E10.5. This is illustrated in ventral views of embryos with the heart removed at E8.5, 9.5, and 10.5 (Figures 1G–I). At E8.5, transgene activity is observed in a population of cells in the dorsal wall of the pericardial cavity and pharyngeal region, which surround the arterial pole of the heart (Figure 1G). By E9.5, bilaterally paired streams of β-galactosidase-positive cells are observed in the pharyngeal region, including cells in the dorsal wall of the pericardial cavity (Figure 1H). By E10.5, almost no expression is observed in the dorsal pericardial wall adjacent to the OFT, whereas the myocardial wall of the arterial pole of the heart is β-galactosidase positive (Figure 1I). A boundary of

[3] Correspondence: rkelly@pasteur.fr (R.G.K.), margab@pasteur.fr (M.E.B.)

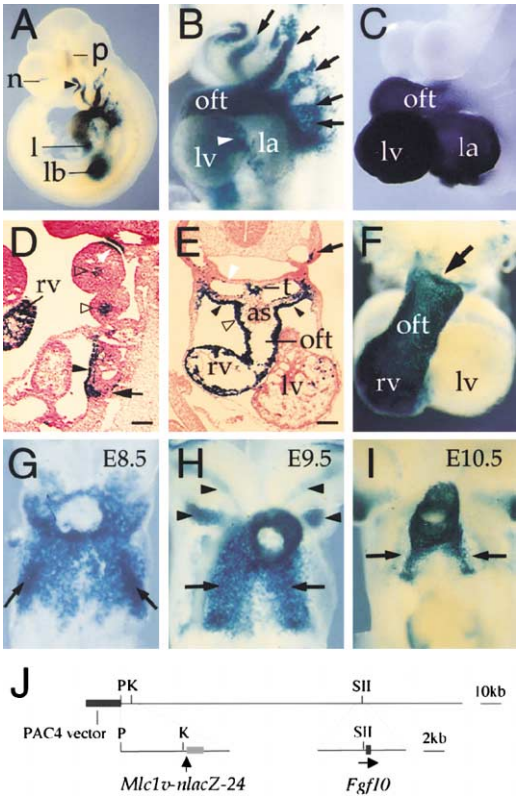

Figure 1. β-Galactosidase Activity of the *Mlc1v-nlacZ-24* Transgene

(A and B) Left lateral views. X-gal incubation at E9.5 reveals β-gal-positive cells in pharyngeal mesoderm of all branchial arches (black arrows), OFT myocardium (oft), limb bud mesenchyme (lb), the developing posterior pituitary (p), nasal placodes (n), first branchial arch ectoderm (black arrowhead), and lung bud mesenchyme (l). Scattered β-gal-positive cells (white arrowhead) are observed in the left ventricle (lv). la, left atrium.

(C) α-*cardiac actin* transcripts accumulate throughout the heart at E9.5.

(D) Sagittal section showing β-gal activity in the dorsal wall of the pericardial cavity (black arrowhead) contiguous to the sixth branchial arch mesoderm (black arrow), the mesodermal core of anterior arches (open arrowheads), and first branchial arch ectoderm (white arrowhead).

(E) Transverse section showing the continuity of β-gal activity from the dorsal wall of the pericardial cavity (black arrowheads) across the aortic sac (open arrowhead) into the myocardial wall of the OFT and embryonic right ventricle (rv). β-Gal activity is also detected in branchial arch mesoderm (black arrow), endothelial cells of the branchial arch arteries (white arrowhead), and the developing thyroid (t) as, aortic sac.

(F) At E11.5, a boundary of transgene expression is observed at the distal end of the OFT (arrow).

(G–I) Ventral views of *Mlc1v-nlacZ-24* embryos with the heart removed, showing β-gal-positive cells in the dorsal wall of the pericardial cavity (arrows) and branchial arches (arrowheads) at E8.5 (G) and E9.5 (H). At E10.5 (I), few β-gal-positive cells (arrows) are observed in the dorsal pericardial wall. The scale bars in (D) and (E) represent 100 μm.

(J) Structure of mouse PAC clone RPCI21 644L10 showing the position of the transgene flanking sequence (gray box) relative to the 5′ exon of *Fgf10* (black box). Arrows indicate the site of integration of the *Mlc1v-nlacZ-24* transgene and the direction of *Fgf10* transcription. P, PI-SceI; K, KpnI; SII, SacII.

transgene expression is observed at the distal end of the OFT at E11.5 (Figure 1F); at this stage, the transformation of epithelial cells into cardiac muscle, as monitored by electron microscopy, is complete (Viragh and Challice, 1973).

The *Mlc1v-nlacZ* transgene contains a truncated mouse *Mlc1v/s* myosin light chain promoter upstream of *nlacZ*. Since the expression pattern of line 24 is specific to one out of four independent founder mice and endogenous *Mlc1v* transcription at E8 and E9.5 is only observed in the myocardium (Lyons et al., 1990), transgene expression is likely to result from a position effect due to regulatory elements at the site of transgene integration; it remains possible, however, that sequences in the *Mlc1v* promoter contribute to myocardial expression. DNA flanking the integration site was isolated using inverse PCR in order to identify candidate genes for the endogenous target of these regulatory elements. A transgene-genomic junction fragment was cloned containing 1.6 kb of genomic DNA sequence adjacent to the integration site. Six hundred bp of unique sequence within this region is homologous to a human DNA sequence contained on a 190 kb BAC (GenBank accession number AC022990) which maps to chromosome 5. The only known gene on this BAC encodes a member of the fibroblast growth factor family of signaling molecules, FGF10. A PAC clone containing the 5′ exon of mouse *Fgf10* (Crackower et al., 1998) also contains the transgene flanking sequence 114 kb 5′ to the ATG of *Fgf10* (Figure 1J). Thus, both human and mouse homologs of the flanking sequence lie upstream of the *Fgf10* gene, which is a candidate target of the regulatory elements trapped by the *Mlc1v-nlacZ-24* transgene.

Fibroblast growth factors are intercellular signaling molecules which function by the activation of transmembrane tyrosine kinase receptors and play multiple key roles in vertebrate embryonic development. During heart development, FGFs expressed in foregut endoderm and precardiac mesoderm have been implicated in cardiomyocyte specification and differentiation (see Lough and Sugi, 2000). *Fgf10* has been reported to be expressed in the adult heart by Northern blot hybridization (Tagashira et al., 1997) and RNase protection analysis (Beer et al., 1997). We investigated whether *Fgf10* was expressed in the heart and pharyngeal region at early stages of mouse development using whole-mount in situ hybridization. *Fgf10* expression was compared with the profile of β-galactosidase activity of the *Mlc1v-nlacZ-24* transgene and the distribution of *nlacZ* transcripts in transgenic embryos.

At E7.5, β-galactosidase activity (Figure 2A) accumulates in anterior mesoderm medially to the earliest differentiating cardiomyocytes marked by α-*cardiac actin* expression (Figure 2E). *Fgf10* transcripts are also expressed in this mesodermal region (Figure 2C), in a highly similar profile to *nlacZ* transcripts in transgenic embryos (Figure 2B). An additional caudal domain of endogenous *Fgf10* expression was observed which is not a site of *Mlc1v-nlacZ-24* transgene expression (Figure 2C, arrows). Transcripts of another FGF gene, *Fgf8*, also accumulate in the region where the *Mlc1v-nlacZ-24* transgene is expressed (Figure 2D; Crossley and Martin, 1995). As the heart tube forms at E8, β-galactosidase activity is observed in a ring at the arterial pole of the

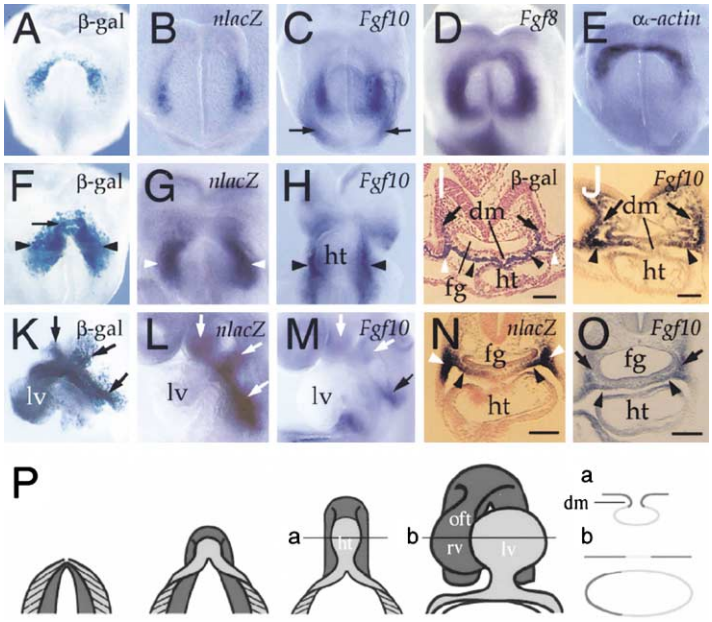

Figure 2. The Expression Pattern of the *Mlc1v-nlacZ-24* Transgene and *Fgf10* from E7.5 to E8.5

(A–E) E7.5, ventral views; X-gal incubation (A); whole-mount in situ hybridization (B–E).

(A) β-gal-positive cells are observed medial to the cardiac crescent.

(B–D) *nlacZ* transcripts in transgenic embryos are observed in a region medial and caudal to the cardiac crescent. *Fgf10* (C) and *Fgf8* (D) are also expressed in this region; an additional caudal domain of *Fgf10* expression is observed (arrows).

(E) α-*cardiac actin* transcripts mark cardiomyocytes within the cardiac crescent.

(F) At E8, β-gal-positive cells are observed at the arterial pole of the heart (arrow) and dorsal to the heart tube (arrowheads).

(G and H) *nlacZ* (G) and *Fgf10* (H) transcripts are observed dorsal to the heart tube (arrowheads).

(I) A transverse section at E8.25 reveals β-gal-positive cells in splanchnic epithelium (black arrowheads) contiguous to anterior mesenchyme (arrows) and adjacent to foregut endoderm (fg), and in somatic mesoderm (white arrowheads). ht, heart tube; dm, dorsal mesocardium.

(J) *Fgf10* transcripts are observed in anterior mesenchyme (arrows) and splanchnic epithelium (arrowheads).

(K) Left lateral view at E8.5 showing β-gal activity in the arterial pole of the heart and pharyngeal mesoderm (arrows); lv, left ventricle.

(L) High-level *nlacZ* transcript accumulation is observed in pharyngeal mesoderm (arrows).

(M) *Fgf10* transcripts are detected in pharyngeal mesoderm (arrows), most strongly in the region of the sixth arch (black arrow).

(N) Transverse section showing *nlacZ* transcripts in pharyngeal, splanchnic (black arrowheads), and somatic mesoderm (white arrowheads), but not in the heart tube (ht). fg, foregut.

(O) *Fgf10* transcripts accumulate in pharyngeal (arrows), somatic, and splanchnic mesoderm (arrowheads). The scale bars represent 50 μm.

(P) Cartoon showing the pattern of β-gal activity of the *Mlc1v-nlacZ-24* transgene during heart tube formation and looping. Dark gray, β-gal-positive cells; hatched, cardiac crescent. Inset: transverse sections at the linear heart tube stage (a) and through the looping heart (b).

heart which is continuous with two domains of expression dorsal to the heart tube (Figure 2F, arrowheads). A transverse section (Figure 2I) shows that the latter β-galactosidase-positive cells are in the medial splanchnic epithelium comprising the dorsal wall of the pericardial cavity. These cells are contiguous to β-galactosidase-positive mesenchymal cells in anterior mesoderm and β-galactosidase-negative myocardial cells within the heart tube; the boundary between transgene-expressing splanchnic mesoderm and nonexpressing myocardial cells is the dorsal mesocardium. At this stage, the distribution of *nlacZ* transcripts is comparable to that of β-galactosidase activity dorsal to the heart tube (Figure 2G); this profile is similar to that of *Fgf10*, which is expressed in anterior mesenchyme and splanchnic epithelium but does not extend as far as the dorsal mesocardium (Figures 2H and 2J).

At E8.5, β-galactosidase activity is observed in the arterial pole of the heart and pharyngeal mesoderm (Figure 2K). *nlacZ* transcripts accumulate predominantly in pharyngeal mesoderm (Figure 2L); *Fgf10* transcripts are also expressed in this region, at a lower level, and are more abundant in mesoderm of the caudal branchial arches (Figure 2M). Both *nlacZ* and *Fgf10* transcripts are observed in splanchnic and somatic mesoderm, in addition to pharyngeal mesenchymal cells (Figures 2N and 2O). In summary, the *Mlc1v-nlacZ-24* transgene is expressed in a bilateral population of *Fgf10*-expressing cells located medial to the cardiac crescent (Figure 2P). During heart tube formation and foregut invagination, these β-galactosidase-positive cells become displaced anteriorly and dorsally relative to the heart tube. Rupture of the dorsal mesocardium and morphogenesis of the pharyngeal region results in the isolation of β-galactosidase-positive cells in the dorsal pericardial wall behind the looping heart tube and the restriction of transgene-expressing cells to branchial arch mesoderm converging on the arterial pole of the heart.

By E9.5, β-galactosidase activity is observed in the myocardial wall of the OFT and embryonic right ventricle, and in a contiguous extracardiac population of pharyngeal mesodermal cells (Figures 1B and 3C). The distribution of *Fgf10* in the mesodermal core of the branchial arches and dorsal pericardial wall at this stage is highly comparable to that of *nlacZ* in *Mlc1v-nlacZ-24* embryos (Figures 3A and 3B). Both transcripts are also observed in the outer curvature of the embryonic right ventricle (Figures 3A and 3B). *Fgf10* is also expressed at a number of other sites of *Mlc1v-nlacZ-24* transgene activity (Figure 3D; compare with Figure 1A). *Fgf10* transcripts do not accumulate in the myocardial wall of the OFT (Figures 3E, 3I, and 3M). Strikingly, *nlacZ* transcripts are also not observed in the distal OFT, but accumulate in branchial arch mesoderm and the dorsal pericardial wall (Figures 3F, 3J, and 3N). In contrast, α-*cardiac actin* is expressed in OFT myocardium, but not the dorsal pericardial wall or pharyngeal mesoderm (Figures 3H and 3L). The lack of *nlacZ* transcripts in the distal OFT

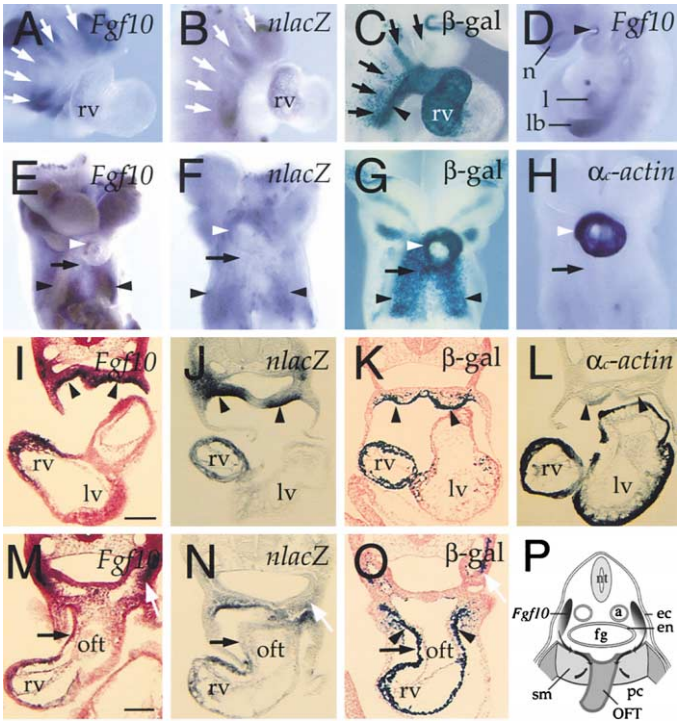

Figure 3. Comparison of *Fgf10* and *nlacZ* Transcripts with β-Galactosidase Activity at E9.5

(A) Right lateral view showing *Fgf10* transcripts in the mesodermal core of the branchial arches (arrows) and right ventricle (rv).

(B) *nlacZ* transcripts are observed in pharyngeal mesoderm (arrows) and the outer curvature of the embryonic right ventricle of *Mlc1v-nlacZ-24* embryos.

(C) β-Gal activity is observed in the right ventricle (rv) and OFT myocardium contiguous to positive cells in the dorsal pericardial wall (arrowhead) and pharyngeal region (arrows).

(D) *Fgf10* is also expressed in limb bud mesenchyme (lb), nasal placodes (n), first branchial arch ectoderm (black arrowhead), and lung bud mesenchyme (l).

(E–H) Ventral views of E9.5 embryos with the hearts removed showing *Fgf10* transcripts (E) in the caudal region of the dorsal pericardial wall (black arrowheads), but not in OFT myocardium (white arrowhead) or adjacent epithelial cells (arrow). This expression profile is similar to that of *nlacZ* transcripts (F) but different from the distribution of β-gal-positive cells (G). α-*cardiac actin* transcripts accumulate in OFT myocardium (white arrowhead) but not the dorsal pericardial wall (arrow) (H).

(I–L) Transverse sections showing *Fgf10* (I) and *nlacZ* (J) transcripts and β-gal-positive cells (K) in the embryonic right ventricle (rv) and dorsal wall of the pericardial cavity (arrowheads). α-*cardiac actin* transcripts are detected throughout the myocardium (L). lv, left ventricle.

(M–O) Transverse sections at the level of the OFT showing that *Fgf10* (M) and *nlacZ* (N) transcripts are not detected in the myocardial wall of the distal OFT (black arrow), whereas β-gal activity (O) is observed in the OFT myocardial wall and aortic sac mesothelium (arrowheads); *Fgf10* and *nlacZ* transcripts and β-gal activity colocalize in pharyngeal mesoderm (white arrows). The scale bars represent 100 μm.

(P) Cartoon showing *Fgf10* expression in anterior mesenchyme in relation to the developing OFT. ec, ectoderm; en, endoderm; sm, splanchnic mesoderm; pc, pericardial cavity; nt, neural tube; a, dorsal aorta; fg, foregut.

of *Mlc1v-nlacZ-24* embryos at E9.5 diverges from the profile of β-galactosidase activity at the same stage (Figures 3G, 3K, and 3O). These data suggest that β-galactosidase activity in the myocardial wall of the OFT and adjacent dorsal pericardial wall reflects accumulated protein in cells which have downregulated transgene transcription, probably reflecting the different half-lives of β-galactosidase and *nlacZ* or *Fgf10* mRNA. β-galactosidase activity may thus provide a pulse-chase readout of transgene transcriptional activity in pharyngeal mesoderm. These observations raise the possibility that a subset of *Fgf10*-expressing cells in pharyngeal mesoderm move from the branchial arch region toward the heart to differentiate as cardiomyocytes, concomitant with the downregulation of *Fgf10* transcription and the rapid elongation of the arterial pole that occurs between E8.5 and E10.5 (Figure 3P).

We investigated whether myocardial precursor cells from the branchial arch region move into the growing arterial pole of the heart during E8 and E9 using DiI labeling. Two series of experiments were carried out involving labeling of extracardiac cells in the pharyngeal region at E8.25 and E9.5, followed in each case by embryo culture for 24 hr. When mesodermal cells dorsal to the heart were labeled at E8.25 by injection through the foregut endoderm, DiI-labeled cells were observed in the proximal OFT after 24 hr (Figures 4A–4D). When cells in the second branchial arch were labeled at E9.5, DiI was observed in the distal OFT after 24 hr (Figures 4E–4H). These results suggest that there is a continuous movement of cells from the pharyngeal region into the arterial pole of the heart between E8.25 and E10.5.

Discussion

The *Mlc1v-nlacZ-24* transgene has integrated 114 kb upstream of *Fgf10* and is expressed in a highly similar pattern to that of *Fgf10* at multiple sites in the embryo, thus behaving like an *Fgf10* enhancer trap. Sites of β-galactosidase activity but not *Fgf10* or *nlacZ* transcript accumulation may be due to differential β-galactosidase and mRNA stability, providing a pulse-chase readout of *Fgf10* transcription. A similar divergence between transcript and protein distribution has been observed for transgenes expressed in the somite (Hadchouel et al., 2000). Our observations suggest that β-galactosidase-positive cells in the distal OFT have downregulated transcription of the transgene, reflecting the downregulation of *Fgf10*, and have moved into this position from pharyngeal mesoderm where high-level transcription and β-galactosidase activity colocalize. Mesenchymal cells in the pharyngeal region are continuous laterally with the splanchnic and somatic mesodermal layers flanking the coelomic cavity and provide a potential source of precursor cells for the splanchnic mesoderm and early heart tube (De Ruiter et al., 1992). Our data suggest that this process continues throughout E8 and E9 to provide precursor cells for the arterial pole of the

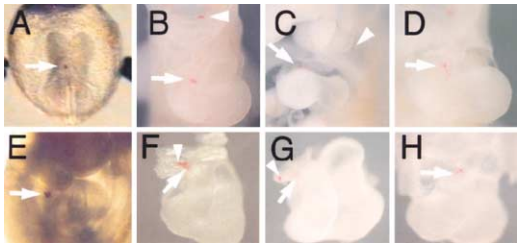

Figure 4. DiI Labeling of Anterior Mesoderm during OFT Elongation

(A–D) Labeling at E8.25.

(A) Video still immediately after DiI label was introduced into mesodermal cells dorsal to the linear heart tube at E8.25 through the anterior intestinal portal (arrow, DiI spot).

(B and C) Ventral (B) and lateral (C) views of the embryo shown in (A) after 24 hr of embryo culture, showing DiI label in the proximal OFT (arrows). Note the DiI-labeled cells in foregut endoderm, which probably correspond to the site of injection (arrowheads).

(D) An additional example shows DiI-labeled cells in the proximal OFT.

(E–H) Labeling at E9.5. Embryo immediately after DiI label was introduced into the second branchial arch through the yolk sac ([E], arrow, DiI spot).

(F–H) Examples of hearts after 24 hr of embryo culture showing DiI-labeled cells in the distal OFT and aortic sac mesothelium (arrows). In (F) and (G), a trail of DiI label from the most ventrally labeled cells back toward the branchial arch region can be observed (arrowheads).

heart. In support of this, DiI labeling shows that there is a progressive movement of cells from distal pharyngeal mesoderm into the growing arterial pole of the heart during E8 and E9. In addition to the OFT, β-galactosidase activity is observed in the embryonic right ventricle, suggesting that the interventricular region is the leading edge of the pharyngeal mesoderm-derived component of the heart. On the basis of these results, we propose that the embryonic heart is composed of cells derived from two myocardial precursor populations—one which gives rise to the early heart tube and inflow region of the heart, and a second population of *Fgf10*-expressing cells in pharyngeal mesoderm which gives rise to the OFT and possibly also the embryonic right ventricle. Such a model is consistent with evidence that the OFT and right ventricle comprise distinct genetic modules of the embryonic heart (Schwartz and Olson, 1999; Bruneau et al., 1999).

Our observations differ fundamentally from those of neural crest cell migration into the OFT with respect to timing, distribution within the pharyngeal region, and the resulting cell types within the heart. Neural crest cells are first observed in the mouse OFT at E9.5 (Jiang et al., 2000; Epstein et al., 2000), whereas *Mlc1v-nlacZ-24*-expressing cells are observed in the arterial pole of the heart from E8. Cardiac neural crest cells migrate predominantly through caudal branchial arches (see Waldo and Kirby, 1999), in contrast to the cell population expressing the *Mlc1v-nlacZ-24* transgene and our DiI labeling results. Furthermore, neural crest cells marked by the expression of a *lacZ* reporter gene activated by a *Wnt1*- or *Pax3*-regulated cre recombinase are excluded from the mesodermal core of the branchial arches, thus showing a reciprocal distribution to that of the *Mlc1v-nlacZ-24* transgene (Jiang et al., 2000; Epstein et al., 2000). Finally, within the heart, neural crest cells give rise to the aorticopulmonary septum rather than the myocardial wall of the OFT (Epstein et al., 2000; Waldo and Kirby, 1999). Despite these basic differences, distal OFT myocardial precursor cells and cardiac neural crest cells are closely apposed in the pharyngeal region between E9.5 and E10.5, and the contribution of these two cell populations to the heart may be coordinated at later stages of OFT development.

Fgf10-expressing cells are positioned medially to the early myocardium, suggesting that regionalization of the embryonic heart along the venous-arterial axis results in part from medial-lateral patterning of cardiac precursors. Zebrafish ventricular precursors lie medial to atrial precursors within the precardiac mesoderm and are the first cells to form the early heart tube (Yelon et al., 1999); these cells express *Fgf8*, which is required for the earliest stages of cardiogenesis, including the induction of *Gata4* and *Nkx2.5* transcription (Reifers et al., 2000). In *Xenopus*, mesoderm medial to that which forms the early heart tube expresses *Nkx2.5* but not downstream cardiac markers (Raffin et al., 2000). While these *Nkx2.5*-expressing cells are fated to become the dorsal pericardial wall and dorsal mesocardium at the linear heart tube stage, our observations suggest that they may contribute to the OFT at later developmental stages.

FGF signaling plays a major role in controlling cell migration including, in *Drosophila*, the directed migration of mesodermal cells to the site at which cardiomyogenesis is activated, a process dependent on the FGF receptor Heartless (see Skaer, 1997). Fgf10 has been shown to control the directed movement and proliferation of epithelia through interactions with other signaling molecules including BMPs and Shh (see Hogan, 1999), and to be involved in the maintenance of stem cell populations (Harada et al., 1999). *Fgf10* null mice exhibit agenesis and dysgenesis of multiple organ systems yet have no reported heart defect, although detailed cardiac morphology has not been described (Min et al., 1998; Sekine et al., 1999; Ohuchi et al., 2000). Overlap between the role of Fgf10 and other FGFs, such as Fgf8, which is expressed in a subset of precardiac mesodermal cells including arterial pole precursor cells (Figure 2D), may rescue arterial pole development in *Fgf10* null mice. Future experiments will address the role of FGF signaling in arterial pole precursor cells and outflow tract morphogenesis.

Experimental Procedures

The *Mlc1v-nlacZ* transgene contains 757 bp upstream of the transcriptional start site, the 5′ UTR and the first 33 codons of the mouse *Mlc1v/s* myosin light chain gene upstream of *nlacZ* (Jerkovic et al., 1997). The promoter contains a 34 bp deletion at −150 relative to the *Mlc1v* transcriptional start site. In line 24, integration has occurred at a single locus containing two to three copies in a head-to-tail array. Transgene expression was monitored by β-galactosidase activity using whole-mount and histological revelation as described by Kelly et al. (1995).

Inverse PCR was carried out using the Expand long template PCR system (Roche) on *Mlc1v-nlacZ-24* DNA ligated at low concentration after SphI digestion. Products larger than a 1.2 kb interrepeat fragment were subcloned into a pGEM-T vector (Stratagene) prior to DNA sequencing. PCR was used to confirm the authenticity of the genomic-transgene junction. DNA sequence analysis was performed using BLAST (Genbank, NCBI), and alignments were carried

out using DNA Strider Version 1.3 (CEA). PAC clones were obtained from BACPAC Resources and mapped using PFG electrophoresis and Southern blot hybridization as described by Hadchouel et al. (2000).

Embryo culture and DiI labeling were performed as described in Franco et al. (2001); labeling at E8.25 was performed through the anterior intestinal portal, and at E9.5 through the visceral yolk sac.

Whole-mount ISH was carried out as described in Zammit et al. (2000), followed by cryostat sectioning. Mouse *Fgf10* and *Fgf8* DNA fragments corresponding to the entire coding sequences were amplified from E11.5 embryo cDNA. PCR products were subcloned into a pGEM-T vector and the sequence was verified. Full-length riboprobes were synthesized using SP6 RNA polymerase and BglII-linearized templates. α-*cardiac actin* and *nlacZ* riboprobes were as described by Sassoon et al. (1988) and Kelly et al. (1995).

Acknowledgments

We are grateful to Diego Franco, Antoon Moorman, and our colleagues in the Buckingham laboratory for critical discussion. This work was supported by grants from the CNRS, Pasteur Institute, and AFM to M.E.B., the BHF (grant number RG 98004) to N.A.B., and the EU Biomed Program (grant number PL964004) to N.A.B. and M.E.B. R.G.K. is an INSERM research fellow and acknowledges prior support from the Amis des Sciences and the FRM.

Received May 18, 2001; revised July 20, 2001.

References

Beer, H.D., Florence, C., Dammeier, J., McGuire, L., Werner, S., and Duan, D.R. (1997). Mouse fibroblast growth factor 10: cDNA cloning, protein characterization, and regulation of mRNA expression. Oncogene *15*, 2211–2218.

Bruneau, B., Logan, M., Davis, N., Levi, T., Tabin, C., Seidman, J., and Seidman, C. (1999). Chamber-specific cardiac expression of *Tbx5* and heart defects in Holt-Oram syndrome. Dev. Biol. *211*, 100–108.

Crackower, M.A., Heng, H.H., and Tsui, L.C. (1998). Assignment of mouse fibroblast growth factor 10 (*Fgf10*) gene to the telomeric region of chromosome 13. Genomics *53*, 247–248.

Crossley, P.H., and Martin, G.R. (1995). The mouse *Fgf8* gene encodes a family of polypeptides and is expressed in regions that direct outgrowth and patterning in the developing embryo. Development *121*, 439–451.

de la Cruz, M.V., Sanchez Gomez, C., Arteaga, M.M., and Arguello, C. (1977). Experimental study of the development of the truncus and the conus in the chick embryo. J. Anat. *123*, 661–686.

De Ruiter, M.C., Poelmann, R.E., Vander Plas-de Vries, I., Mentink, M.M., and Gittenberger-de Groot, A.C. (1992). The development of the myocardium and endocardium in mouse embryos. Fusion of two heart tubes? Anat. Embryol. *185*, 461–473.

Epstein, J.A., Li, J., Lang, D., Chen, F., Brown, C.B., Jin, F., Lu, M.M., Thomas, M., Liu, E., Wessels, A., and Lo, C.W. (2000). Migration of cardiac neural crest cells in *Splotch* embryos. Development *127*, 1869–1878.

Fishman, M.C., and Chien, K.R. (1997). Fashioning the vertebrate heart: earliest embryonic decisions. Development *124*, 2099–2117.

Franco, D., Kelly, R., Moorman, A.F.M., Lamers, W.H., Buckingham, M., and Brown, N.A. (2001). *MLC3F* transgene expression in *iv* mutant mice reveals the importance of left-right signalling pathways for the acquisition of left and right atrial but not ventricular compartment identity. Dev. Dyn. *221*, 206–215.

Hadchouel, J., Tajbakhsh, S., Primig, M., Chang, T.H., Daubas, P., Rocancourt, D., and Buckingham, M. (2000). Modular long-range regulation of *Myf5* reveals unexpected heterogeneity between skeletal muscles in the mouse embryo. Development *127*, 4455–4467.

Harada, H., Kettunen, P., Jung, H.S., Mustonen, T., Wang, Y.A., and Thesleff, I. (1999). Localization of putative stem cells in dental epithelium and their association with Notch and FGF signaling. J. Cell Biol. *147*, 105–120.

Hogan, B.L. (1999). Morphogenesis. Cell *96*, 225–233.

Jerkovic, R., Vitadello, M., Kelly, R., Buckingham, M., and Schiaffino, S. (1997). Fibre type-specific and nerve-dependent regulation of myosin light chain 1 slow promoter in regenerating muscle. J. Muscle Res. Cell Motil. *18*, 369–373.

Jiang, X., Rowitch, D.H., Soriano, P., McMahon, A.P., and Sucov, H.M. (2000). Fate of the mammalian cardiac neural crest. Development *127*, 1607–1616.

Jones, C.M., Lyons, K.M., and Hogan, B.L. (1991). Involvement of *Bone Morphogenetic Protein-4* (*BMP-4*) and *Vgr-1* in morphogenesis and neurogenesis in the mouse. Development *111*, 531–542.

Kelly, R., Alonso, S., Tajbakhsh, S., Cossu, G., and Buckingham, M. (1995). Myosin light chain 3F regulatory sequences confer regionalised cardiac and skeletal muscle expression in transgenic mice. J. Cell Biol. *129*, 383–396.

Lough, J., and Sugi, Y. (2000). Endoderm and heart development. Dev. Dyn. *217*, 327–342.

Lyons, G.E., Schiaffino, S., Sassoon, D., Barton, P., and Buckingham, M. (1990). Developmental regulation of myosin gene expression in mouse cardiac muscle. J. Cell Biol. *111*, 2427–2436.

Min, H., Danilenko, D.M., Scully, S.A., Bolon, B., Ring, B.D., Tarpley, J.E., DeRose, M., and Simonet, W.S. (1998). *Fgf-10* is required for both limb and lung development and exhibits striking functional similarity to *Drosophila branchless*. Genes Dev. *12*, 3156–3161.

Ohuchi, H., Hori, Y., Yamasaki, M., Harada, H., Sekine, K., Kato, S., and Itoh, N. (2000). FGF10 acts as a major ligand for FGF receptor 2 IIIb in mouse multi-organ development. Biochem. Biophys. Res. Commun. *277*, 643–649.

Raffin, M., Leong, L.M., Rones, M.S., Sparrow, D., Mohun, T., and Mercola, M. (2000). Subdivision of the cardiac Nkx2.5 expression domain into myogenic and nonmyogenic compartments. Dev. Biol. *218*, 326–340.

Reifers, F., Walsh, E.C., Leger, S., Stainier, D.Y., and Brand, M. (2000). Induction and differentiation of the zebrafish heart requires fibroblast growth factor 8 (*fgf8*/*acerebellar*). Development *127*, 225–235.

Sassoon, D., Garner, I., and Buckingham, M. (1988). Transcripts of α-cardiac and α-skeletal actins are early markers for myogenesis in the mouse embryo. Development *104*, 155–164.

Sekine, K., Ohuchi, H., Fujiwara, M., Yamasaki, M., Yoshizawa, T., Sato, T., Yagishita, N., Matsui, D., Koga, Y., Itoh, N., and Kato, S. (1999). Fgf10 is essential for limb and lung formation. Nat. Genet. *21*, 138–141.

Schultheiss, T.M., Burch, J.B., and Lassar, A.B. (1997). A role for bone morphogenetic proteins in the induction of cardiac myogenesis. Genes Dev. *11*, 451–462.

Schwartz, R.J., and Olson, E.N. (1999). Building the heart piece by piece: modularity of *cis*-elements regulating *Nkx2-5* transcription. Development *126*, 4187–4192.

Skaer, H. (1997). Morphogenesis: FGF branches out. Curr. Biol. *7*, R238–R241.

Tagashira, S., Harada, H., Katsumata, T., Itoh, N., and Nakatsuka, M. (1997). Cloning of mouse FGF10 and up-regulation of its gene expression during wound healing. Gene *197*, 399–404.

Viragh, S., and Challice, C.E. (1973). Origin and differentiation of cardiac muscle cells in the mouse. J. Ultrastruct. Res. *42*, 1–24.

Waldo, K., and Kirby, M.L. (1999). Development of the great arteries. In Living Morphogenesis of the Heart, M.V. de la Cruz and R.R. Markwald, eds. (Boston: Birkhauser), pp. 187–217.

Yelon, D., Horne, S.A., and Stainier, D.Y. (1999). Restricted expression of cardiac myosin genes reveals regulated aspects of heart tube assembly in zebrafish. Dev. Biol. *214*, 23–37.

Zammit, P.S., Kelly, R.G., Franco, D., Brown, N., Moorman, A.F., and Buckingham, M.E. (2000). Suppression of atrial myosin gene expression occurs independently in the left and right ventricles of the developing mouse heart. Dev. Dyn. *217*, 75–85.